Improvement of high velocity impact performance of carbon nanotube and lead reinforced magnesium alloy

M.F. Abdullah[2,a], S. Abdullah[1,b*], N.A. Rahman[1], M.S. Risby[2], M.Z. Omar[1] and Z. Sajuri[1]

[1]Department of Mechanical and Materials Engineering,
Faculty of Engineering & Built Environment,
Universiti Kebangsaan Malaysia.
43600 UKM Bangi, Selangor, Malaysia
[2]Department of Mechanical Engineering, Faculty of Engineering,
Universiti Pertahanan Nasional Malaysia,
Kem Sg. Besi 57000 Kuala Lumpur, Malaysia.
Email: [a]m.faizal@upnm.edu.my, [b]shahrum@ukm.edu.my

ABSTRACT

This paper presented the effect of strain rate changes due to Carbon Nanotube (CNT) and Lead addition in Magnesium Alloy, AZ31B on high velocity impact performance. This metal is normally used to fabricate armored vehicle panel. The changing strain will affect the strain rate and had been widely used in automotive applications to accommodate high velocity impact. High strain rate material was applied on the armored vehicle to withstand the impact of the projectile. AZ31B alloy was reinforced with CNT and Lead using Disintegrated Melt Deposition (DMD) method. AZ31B ingots were melted at a temperature of 660 ºC and produced the reinforcement of CNT and Lead during the melting process. Mixed materials were completely inserted into the mold for further process. Microstructure analysis was performed to observe the variance structure of samples. The high velocity impact experiment was performed using a Split Hopkinson Pressure Bar machine. The diameter of the sample was 18 mm with 12.5 mm thickness. The addition of materials such as CNT and Lead into AZ31B had increased the material strain rate. The effect of increasing the strain rate was in line with the increase of energy absorption. The result showed that the strain rate had increased about 30% from the original material, AZ31B and consequently also increased the energy absorption. Thus, the addition of CNT and Lead would increase the strain rate of the original material of magnesium alloy and hence increase the energy absorption capability during impact.

Keywords: CNT, High velocity impact, Lead, Magnesium Alloy, Strain rate.

INTRODUCTION

Recent technology development in automotive field requires lightweight material which is high in strength. Exploration of new materials has a high impact in the study of change in strain, especially when subjected to high velocity impact [1-3]. Changing strain at high velocity impact affects the material's energy absorption and prevents the occurrence of fracture failure [4-7]. The magnesium alloy is characterized as a lightweight material and has high energy absorption capability. Magnesium alloys can naturally withstand impacts effectively because of their unique combination of high tensile strength, low density, and

superior shock absorbency which are 100 times greater than that of ordinary aluminum alloys [5, 8, 9]. Split Hopkinson Pressure Bar (SHPB) was modernized by Herbert Kolsky in 1949 [10, 11] and is applicable to high velocity impact for high strain rate testing [2, 4, 5]. Amanda et al. [12] used the SHPB in studying the mechanical response of CNT in fabric composite. Researches on SHPB had been done to study the durability of magnesium alloy, AZ31B at a high strain rate [13, 14]. According to Nguyen and Gupta [15], addition of reinforced materials such as CNT in the original material can increase the material's strain rate. Besides CNT, the reinforcement of lead (Pb) into the original material can also enhance the material's properties of magnesium alloy [16, 17]. Elastic properties of Pb improve the ductility of the material during impact. The reinforcement of CNT and Pb can increase the strain rate of the material being studied.

Magnesium alloy, AZ31B has high energy absorption capability; however, it has the disadvantage of low ductility. The addition of reinforced material can affect the change in strain rate and material properties. The strength of the material closely affects the change in strain, especially if that material can accommodate the high velocity impact. The objective of this study was to observe the effects of changing strain on the material AZ31B with the reinforcement of Lead and CNT under a high velocity impact. These additions affected the structure of magnesium alloy, AZ31B on the strain rate which resulted in the improved material properties of magnesium alloy in terms of high velocity impact.

EXPERIMENTAL SET UP

This study was executed in accordance to the flow diagram as shown in Figure 1. Three different materials were chosen for this study which were AZ31B, AZ31B + 5% Pb and AZ31B +0.1% CNT + 5% Pb. These materials were tested using SHPB to get the strain behaviour on materials under high velocity impact.
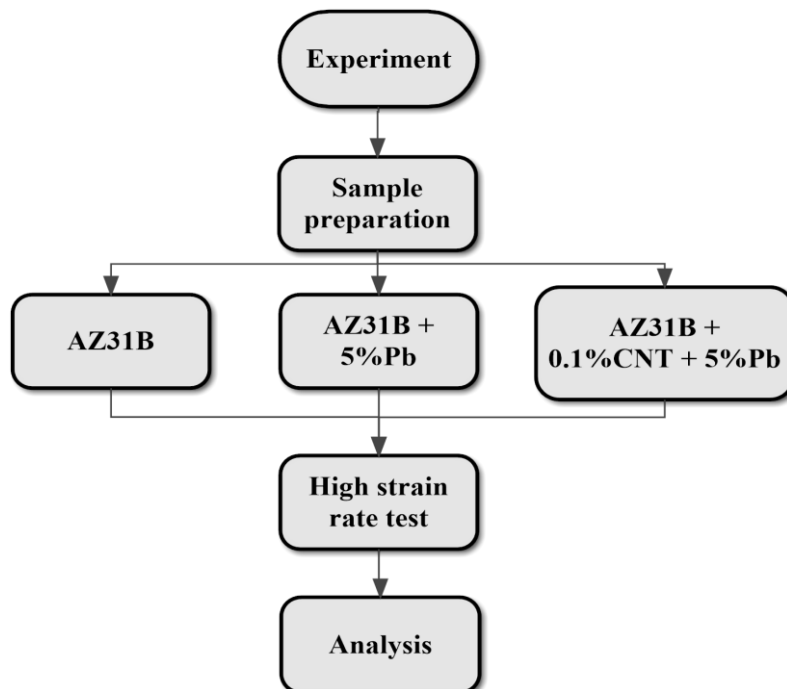

Figure 1: Flow diagram of the experimental procedure

Sample preparation

A mixture of magnesium alloy, AZ31B with CNT and Pb were prepared using an induction furnace. The ingot type for magnesium alloy, AZ31B was used. The reinforcement of materials into AZ31B was based on the weight percentage of Lead (Pb) and CNT materials. The CNT had an outer diameter of 10-30 nm, the density was 2.1 g/cm^3 and it contained more than 90% purity. The Lead powder added contained 99.9% purity with the density of 11.34 g/cm^3. The process of reinforcement materials into the AZ31B utilized the Disintegrated Melt Deposition (DMD) method by which the ingot AZ31B was heated to the melting temperature. Heating process was done in the chamber that was partly vacuum and Argon gas was induced into the combustion chamber at 25 mm/min. The function of Argon gas was to avoid the oxidization process of magnesium when it was melting. After the ingot was completely melted, the composition of CNT and Lead were added into the chamber through the pipeline chamber. One specimen of AZ31B was reinforced with 5% of Pb and another specimen was reinforced with 0.1% CNT and 5% Pb. Mixture of magnesium alloy will be the input onto the mold cavity with the size of 200 mm in length x 100 mm in width x 25 mm in thickness. Figure 2 shows the induction furnace machine that was used for the reinforcement process.
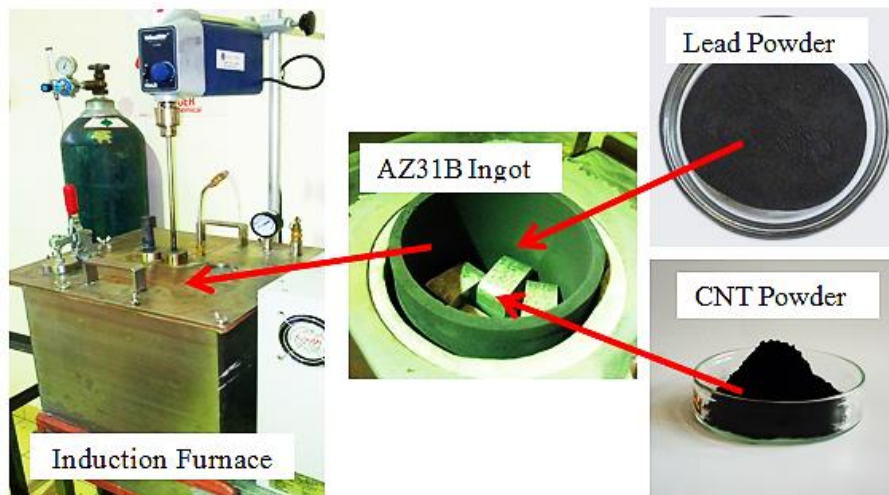

Figure 2. Induction furnace for melting magnesium alloy and reinforcement materials.
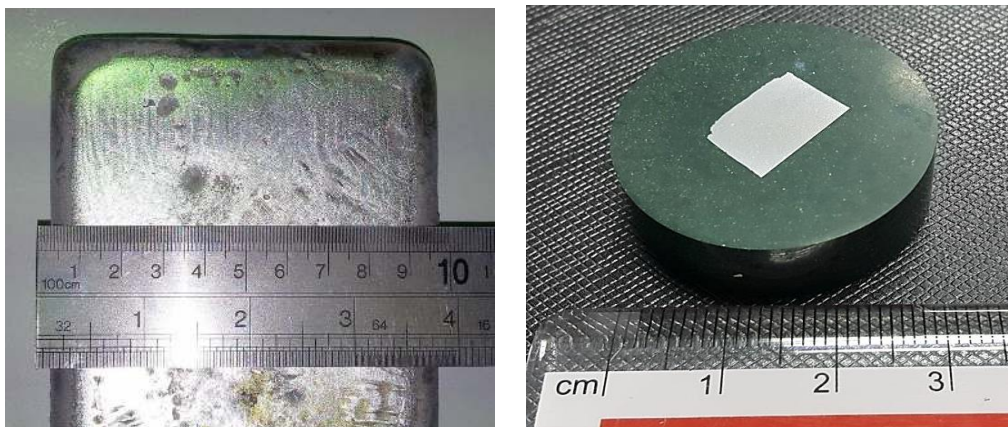

Figure 3. (a) Raw sample after DMD process; (b) Sample preparation for microstructure investigation.

Microstructure Observation

After different compositions of Pb and CNT were added to the AZ31B samples, Figure 3(a) shows the raw sample after the DMD process before the sample was cut into different shapes of the sample test. Figure 3(b) shows how the microstructure of the samples was studied. The samples were grounded, polished, and etched to obtain clearer images of the grain boundaries under a microscope. High magnification was used to observe the grain boundaries of the structure.

Split Hopkinson pressure bar preparation

Figure 4 shows a schematic of the basic Hopkinson bar setup. It consisted of two long cylindrical bars of the same diameter called as incident and transmitted bars. In a compression test, the sample sat sandwiched between the incident and transmitted bars. A striker bar of the same diameter was propelled using a gas gun, that it struck the incident bar squarely on the end. This generated a compression wave which travelled down the incident bar. Part of the wave was reflected and another part was transmitted through the interface with the specimen. The stress pulse continued through the specimen and into the transmitted bar. The incident stress pulse and transmitted stress pulse were measured in real-time using strain gauges on the incident and transmitted bars. If the two bars remained elastic and wave dispersion was ignored, then the measured stress pulses can be assumed to be the same ones acting on the sample.
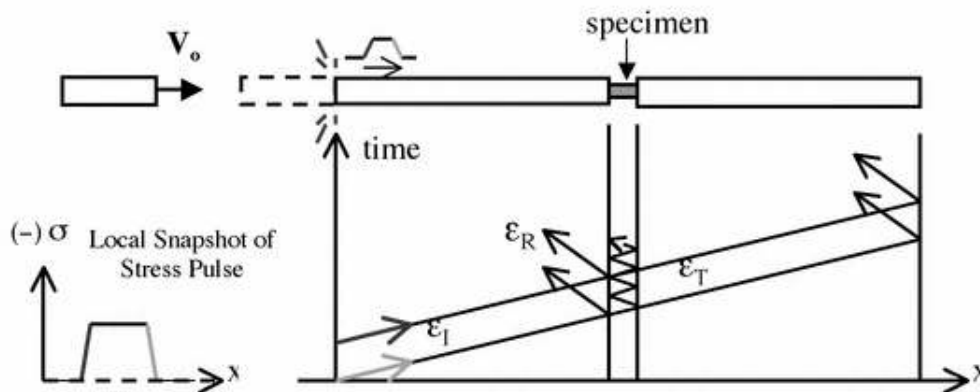

Figure 4. Schematic of the Split Hopkinson Pressure Bar setup [16].

Elastic wave propagation in a cylinder during the experimental SHPB can be described by a one-dimensional elastic wave equation. Instead, a one-dimensional elastic wave equation was used to get the stress and strain in the specimen [18]. The stress, strain and strain rate were calculated based on the incident bar and transmitter bar during compression experiments. The equations involved are shown as follows [10, 12, 14, 18]:

$$\sigma_s(t) = E \frac{A_b}{A_s} \varepsilon_t(t) \tag{1}$$

$$\varepsilon_s = -\frac{2C_0}{L} \int_0^t \varepsilon_r(t)dt \tag{2}$$

$$\bar{\varepsilon}_s = \frac{d\varepsilon(t)}{dt} = \frac{-2C_0}{L} \varepsilon_r(t) \tag{3}$$

where A, E and C_0 are a cross-sectional area, Young's modulus and the wave velocity bar, respectively. L and A refer to the length and cross-sectional area of the sample. ε_r (t) and ε_t (t) show the axial strain on the reflected pulse and transmitter pulse, where the measurement took into account the function of time.

The SHPB tool used a 20 mm diameter high strength aluminum and the length of the incident bar and the transmitted bar were 2000 mm and 2500 mm, respectively. Striker bar (bullet) used was 200 mm in length. The specimen size for this experiment was 18 mm in diameter and 12.5 mm in thickness. The experiment conducted followed the standard by The American Society of Mechanical Engineers (ASME) [18]. The velocity of striker bar was recorded as 20 m/s. The SHPB used is shown in Figure 5. Strain gauge was mounted on the incident bar and the transmission bar for capturing strain data and data acquisition was used at a frequency of 1.0kHz.
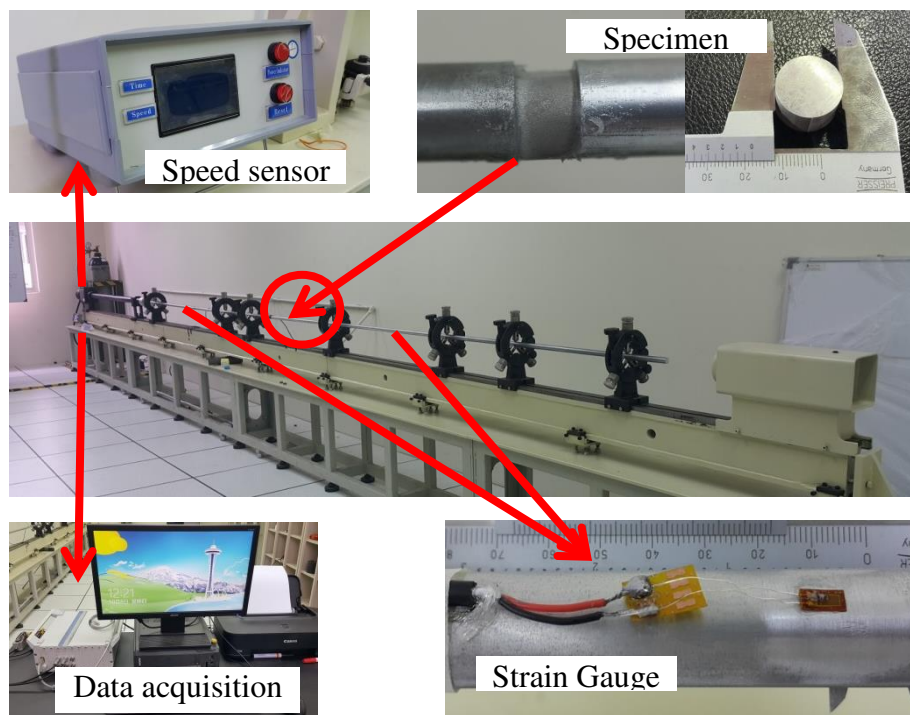

Figure 5. Split Hopkinson Pressure bar apparatus.
.

RESULTS AND DISCUSSION

Figure 6 shows the microstructures of AZ31B samples with different Pb and CNT compositions. The visible grain boundaries of each combination mixture differed. The grain boundary of AZ31B + 0.1%CNT + 5%Pb was larger than that of AZ31B and added 5%Pb. The AZ31B and AZ31B +5%Pb was more on the martensite phase and it was the hardest and strongest and, in addition, the most brittle; it had, in fact, negligible ductility. Figure 7 shows the strain incident bar data produced from the SHPB data acquisition system and Figure 8 shows the strain transmitted bar from the SHPB data acquisition system. The responses obtained were ε_i, ε_r and ε_t which indicated the incident strain pulse, reflected strain pulse and transmitted strain pulse, respectively. Compare to Amanda et al,'s [12]study, the patents of the response of the incident strain pulse, reflected strain pulse and transmitted strain pulse were similar. However, Amanda et al,'s [12] study had focused on the speed range of 10 m/s to 15 m/s. Figure 9 shows the stress of materials

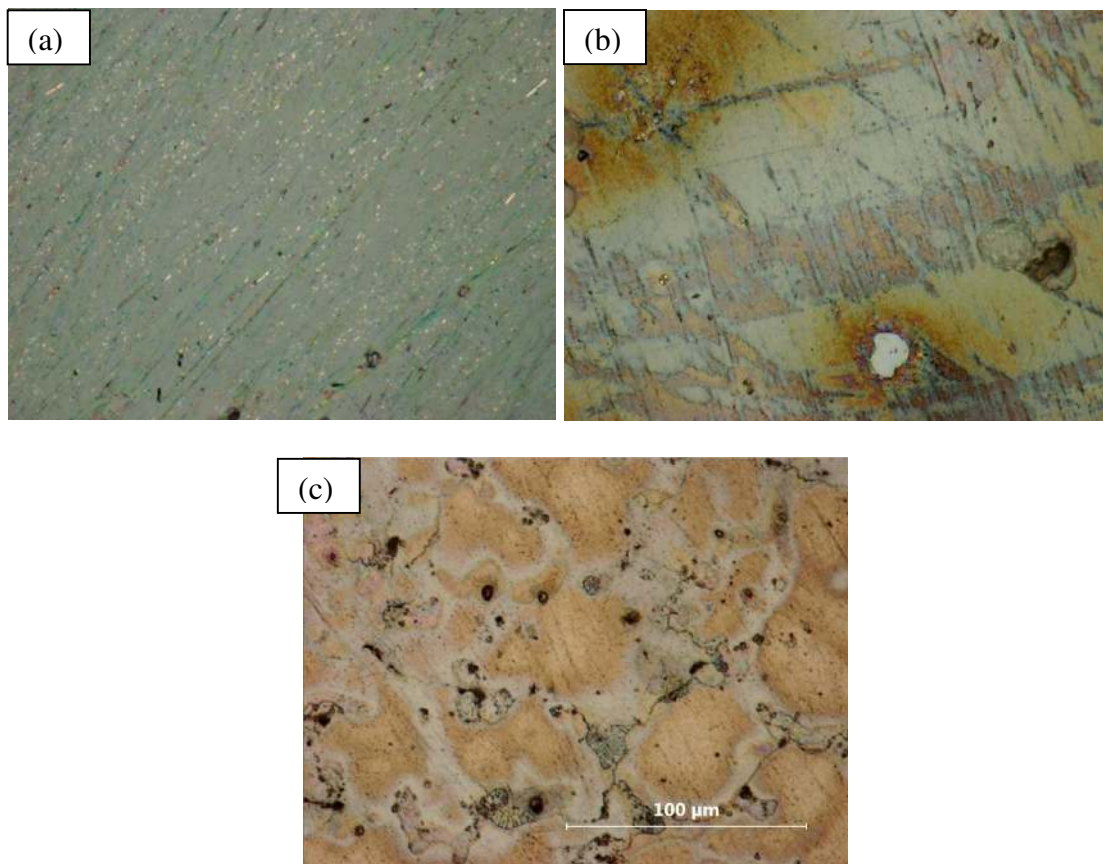using Eq. (1). The trend for each reinforced AZ31B material was similar to the original AZ31B response.

Figure 6. Microstructure of sample in magnification of 100 µm:
(a) AZ31B, (b) AZ31B + 5% Pb, (c) AZ31B + 0.1%CNT + 5%Pb.
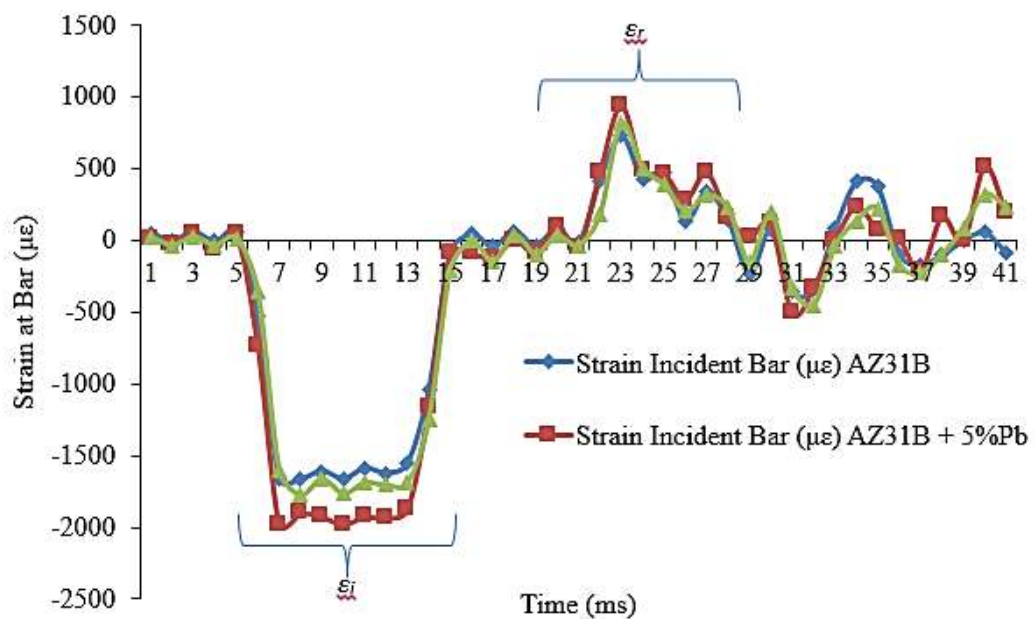

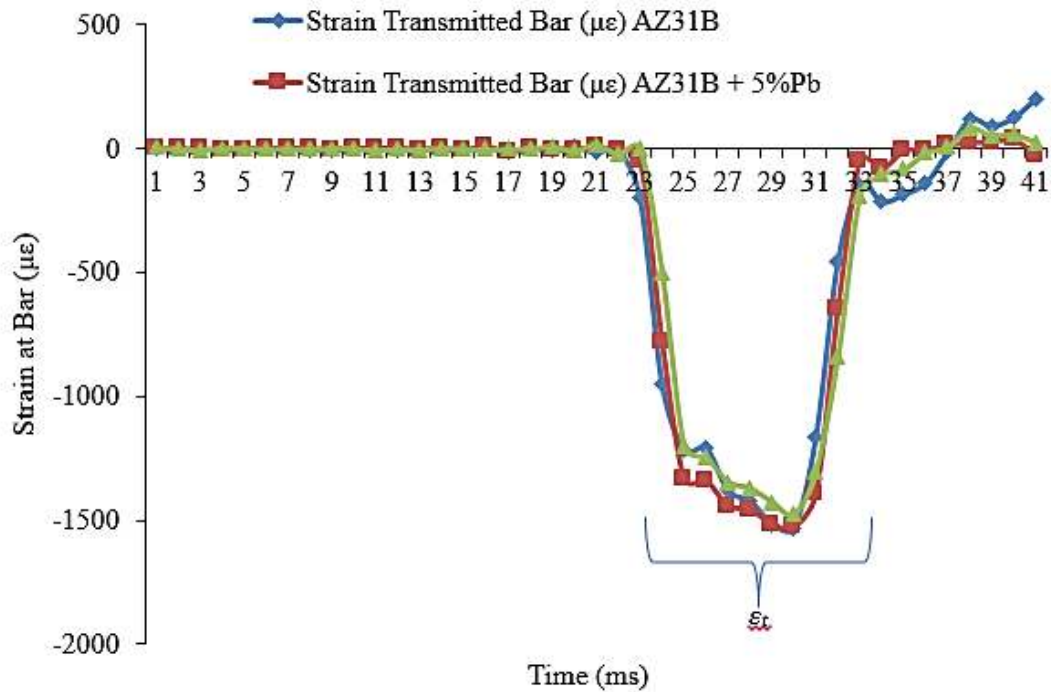Figure 7. Strain incident bar from compression Split Hopkinson pressure bar test.

Figure 8. Strain transmitted bar from compression Split Hopkinson pressure bar test.
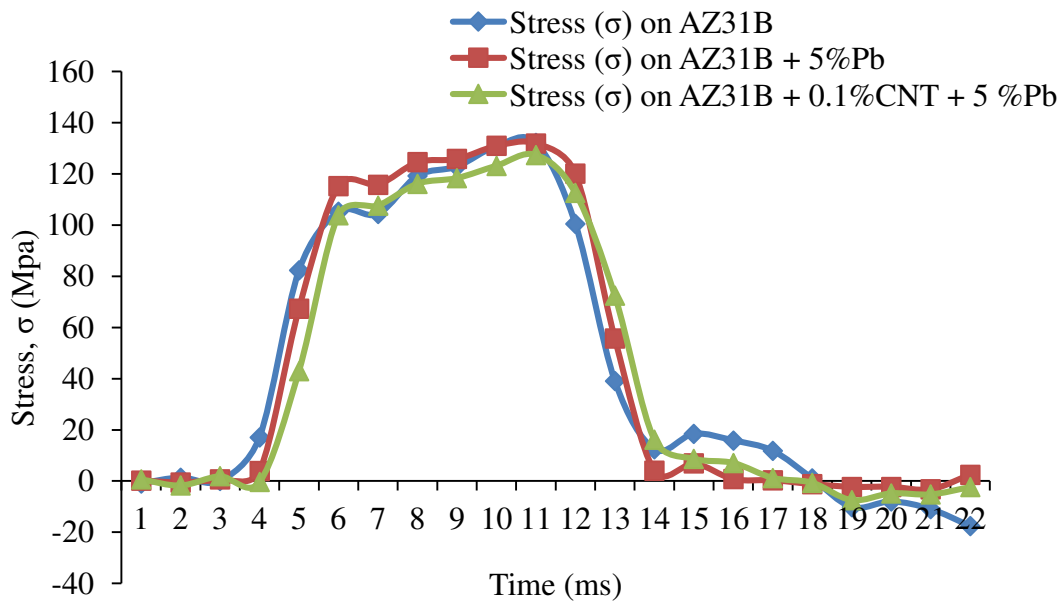

Figure 9. Applied stress on each material tested.

Figure 10 shows the strain of specimens using Eq. (2) as a function of time. From Figure 11 it can be seen that AZ31B has the highest strain which is 9617.64. Reinforced AZ31B + 5% Pb and AZ31B + 0.1% CNT + 5% Pb have reductions in strain at 3.79% and 7.01%, respectively. From Figure 11 as derived from Eq. (3), obtained was the range of strain rate for each specimen which were AZ31B, AZ31B + 5% Pb and AZ31B + 0.1% + 5% Pb CNT at 864.26 s^{-1}, 1141.80 s^{-1} and 996.57 s^{-1}, respectively. Therefore, the

percentages of increment of strain rate for AZ31B + 5% Pb and AZ31B + 0.1% CNT + 5% Pb were 32.11% and 15.31%, respectively. Increasing the strain rate affected the energy absorption of materials which can be observed in Figure 10's stress-strain curve for high impact materials.
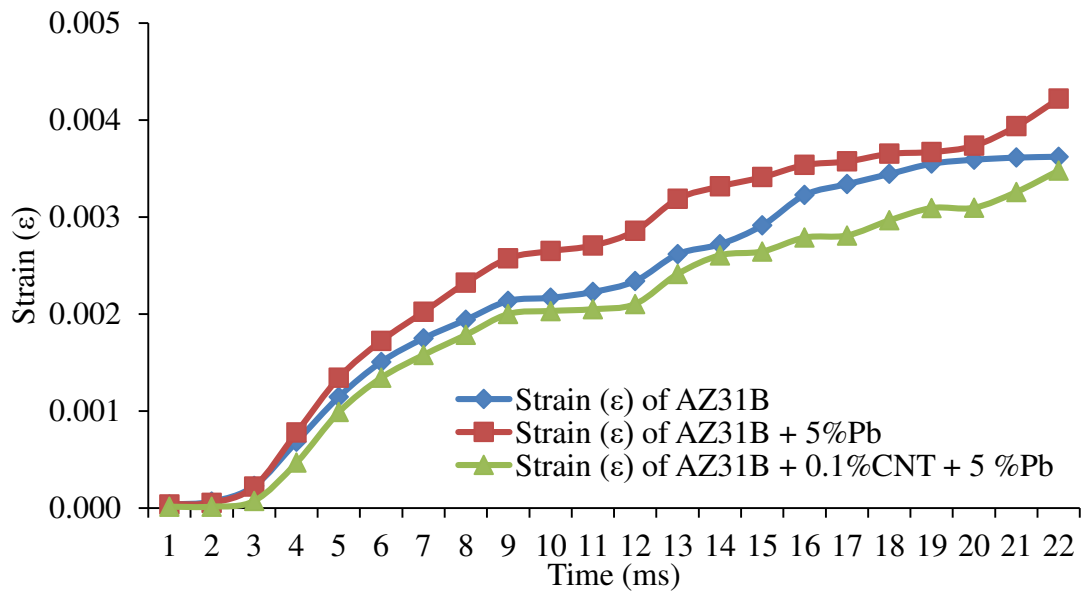
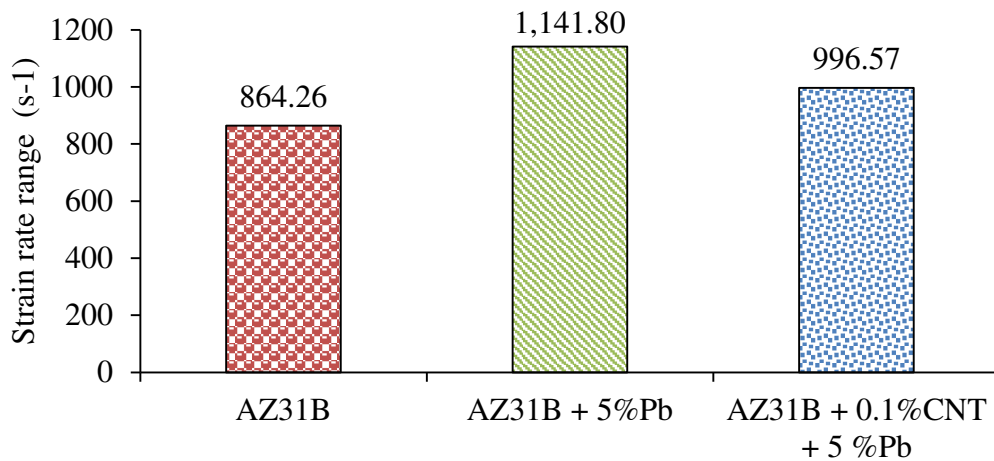Figure 10. The applied strain of materials tested.

Figure 11. The strain rate range of materials tested.

Energy absorption was calculated based on the area under the curve [8-11]. From Figure 12, energy absorption evaluated for AZ31B, AZ31B + 5% Pb and AZ31B + 0.1% CNT + 5% Pb are 938.98 kJ, 1019.05 kJ and 902.79 kJ, respectively. Figure 13 shows the energy absorption under the stress-strain graph. The energy absorption for AZ31B + 5% Pb increased at 8.53%, but for AZ31B + 0.1% CNT + 5% Pb it decreased at the percentage of 3.85%. This situation showed that energy absorption was affected by the change in strain and strain rate of materials. From the analysis, the reinforcement materials into AZ31B changed the strain rate and energy absorption of materials. AZ31B + 5% Pb gave the highest increase in terms of strain rate and energy absorption compared to AZ31B + 0.1% and CNT + 5% Pb. This happened because of the composition of CNT

reinforced which had not achieved an optimal level and this had led to a weak material structure to structural failure [3, 14, 19, 20]. However, the reinforcement of materials into AZ31B gave positive effects of attenuating in high velocity impact. This alloy material could be used for armored vehicles. At the same time, this study showed the effectiveness of the new composition of magnesium alloy. This material had the properties of ballistic resistance which gave an advantage in the maneuverability of armored vehicles.
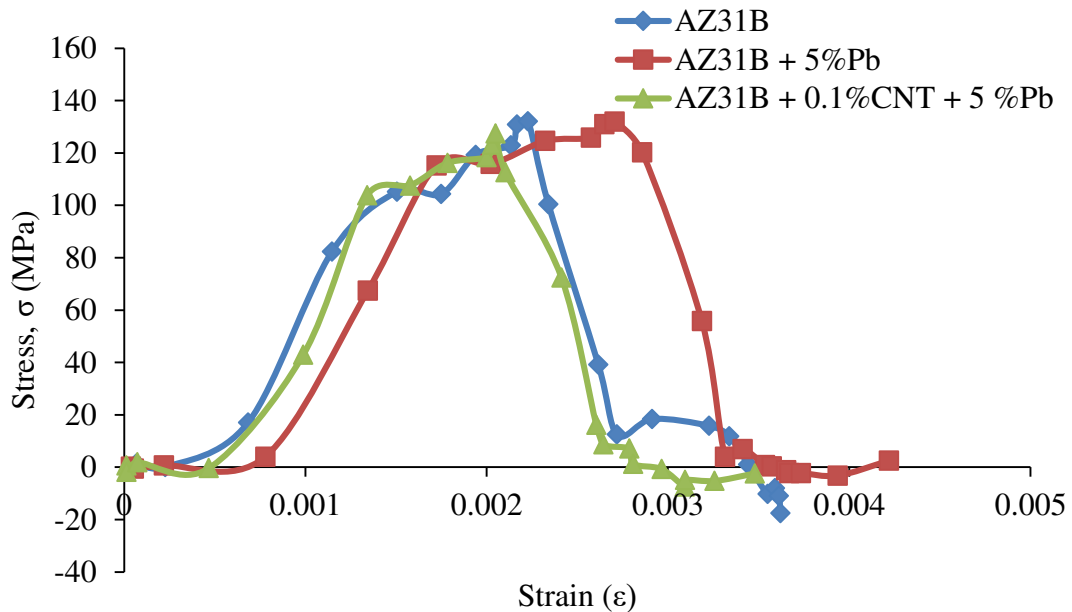

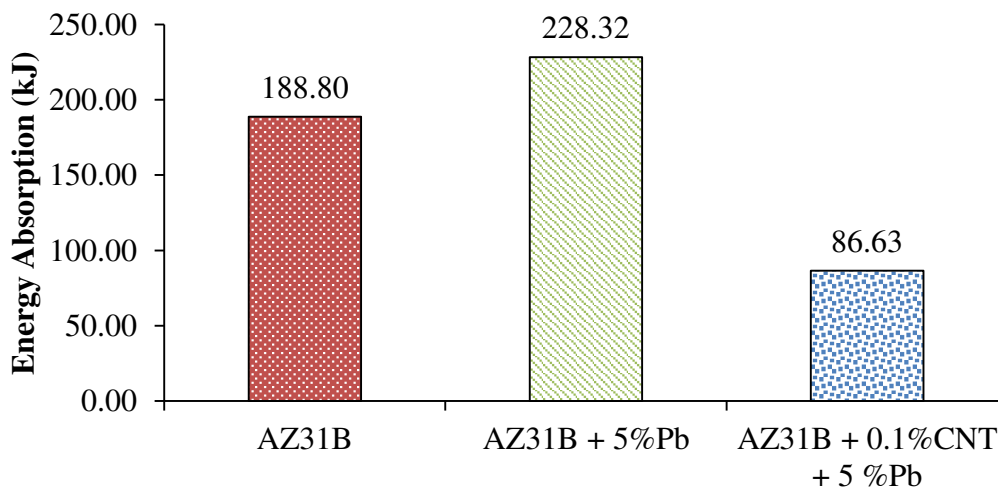Figure 12. Stress-strain curve of materials during the Split Hopkinson pressure bar test.

Figure 13. Energy absorption of materials testing.

CONCLUSIONS

The reinforcement materials such as CNT and Pb into AZ31B affected the strain rate and energy absorption of AZ31B under high velocity impact. The reinforcement materials increased the strain rate of AZ31B up to 30% from the original. Increasing the strain rate affected the energy absorption of materials by 20% from the original. The energy absorption of additional CNT was lower than that of the original AZ31B alloy. This result

indicated that the addition of CNTs affected the blank voids to be filled by the CNTs which will avoid the dislocation process. CNT content was not enough to cause an uneven internal structure of magnesium, which was susceptible to each molecule sliding. This also interfered with the van der Waals bond, which made CNT weaker, because the voids in the molecules were magnesium alloy. The nature of strain rate on these materials was very important in assessing the ability of the material properties, especially in selecting materials capable to withstand high velocity impact. However, combination and percentage composition were not optimum and gave a negative effect to the material properties. It caused the formation of weak material structure to structural failure. Furthermore, magnesium alloy can be the substance used for high velocity impact and it is highly recommended in the application of armored vehicles in a military vehicle. This is because armored vehicles are subjected to the penetration of high velocity projectile impact.

ACKNOWLEDGEMENTS

REFERENCES

[1]   Naik N, Ch V, Kavala VR. Hybrid composites under high strain rate compressive loading. Materials Science and Engineering: A. 2008;498:87-99.

[2]   Li Z, Lambros J. Determination of the dynamic response of brittle composites by the use of the split Hopkinson pressure bar. Composites Science and Technology. 1999;59:1097-107.

[3]   Xiao J, Shu DW. Compressive behavior and constitutive analysis of AZ31B magnesium alloy over wide range of strain rates and temperatures. Metals and Materials International. 2015;21:823-31.

[4]   Chen R, Xia K, Dai F, Lu F, Luo S. Determination of dynamic fracture parameters using a semi-circular bend technique in split Hopkinson pressure bar testing. Engineering Fracture Mechanics. 2009;76:1268-76.

[5]   Jones TL, DeLorme RD, Burkins MS, Gooch WA. Ballistic evaluation of magnesium alloy AZ31B. DTIC Document; 2007.

[6]   Asgari H, Odeshi A, Szpunar J, Zeng L, Olsson E. Grain size dependence of dynamic mechanical behavior of AZ31B magnesium alloy sheet under compressive shock loading. Materials Characterization. 2015;106:359-67.

[7]   Ghazali FA, Manurung YHP, Mohamed MA, Alias SK, Abdullah S. Effect of process parameters on the mechanical properties and failure behavior of spot welded low carbon steel. Journal of Mechanical Engineering and Sciences. 2015;8:1489-97.

[8]   Múgica J, Aretxabaleta L, Ulacia I, Aurrekoetxea J. Impact characterization of thermoformable fibre metal laminates of 2024-T3 aluminium and AZ31B-H24 magnesium based on self-reinforced polypropylene. Composites Part A: Applied Science and Manufacturing. 2014;61:67-75.

[9]   Nafsin N, Rashed HMMA. Effects of copper and magnesium on phase formation modeling and mechanical behavior in AL-CU-MG alloys. International Journal of Automotive and Mechanical Engineering. 2013;8:1151-61.

[10]   Omar MF, Akil HM, Ahmad ZA, Mazuki A, Yokoyama T. Dynamic properties of pultruded natural fibre reinforced composites using Split Hopkinson Pressure Bar technique. Materials & Design. 2010;31:4209-18.

[11]   Matadi R, Hablot E, Wang K, Bahlouli N, Ahzi S, Avérous L. High strain rate behaviour of renewable biocomposites based on dimer fatty acid polyamides and cellulose fibres. Composites Science and Technology. 2011;71:674-82.

[12]   Lim AS, An Q, Chou T-W, Thostenson ET. Mechanical and electrical response of carbon nanotube-based fabric composites to Hopkinson bar loading. Composites Science and Technology. 2011;71:616-21.

[13]   Mukai T, Mohri T, Mabuchi M, Nakamura M, Ishikawa K, Higashi K. Experimental study of a structural magnesium alloy with high absorption energy under dynamic loading. Scripta Materialia. 1998;39:1249-53.

[14]   Sanjari M, Farzadfar A, Sakai T, Utsunomiya H, Essadiqi E, Jung I-H, et al. A texture and microstructure analysis of high speed rolling of AZ31 using split Hopkinson pressure bar results. Journal of Materials Science. 2013;48:6656-72.

[15]   Nguyen Q, Gupta M. Increasing significantly the failure strain and work of fracture of solidification processed AZ31B using nano-Al 2 O 3 particulates. Journal of Alloys and Compounds. 2008;459:244-50.

[16]   Srinivasan A, Pillai U, Pai B. Effect of Pb addition on ageing behavior of AZ91 magnesium alloy. Materials Science and Engineering: A. 2007;452:87-92.

[17]   Gupta M, Wong W. Magnesium-based nanocomposites: Lightweight materials of the future. Materials Characterization. 2015;105:30-46.

[18]   SHPB. A.s., Split- Hopkinson Pressure Bar Apparatus. Texas2006.

[19]   Soliman EM, Sheyka MP, Taha MR. Low-velocity impact of thin woven carbon fabric composites incorporating multi-walled carbon nanotubes. International Journal of Impact Engineering. 2012;47:39-47.

[20]   Staroselsky A, Anand L. A constitutive model for hcp materials deforming by slip and twinning: application to magnesium alloy AZ31B. International Journal of Plasticity. 2003;19:1843-64.